Influence of ball milling on CaO crystal growth during limestone and dolomite calcination: Effect on CO_2 capture at Calcium Looping conditions.

Pedro E. Sánchez-Jiménez[1,], José M. Valverde[2], Antonio Perejón[1,3], Antonio de la Calle[1, 2] , Santiago Medina[4] and Luis A. Pérez-Maqueda[1]*

[1] Instituto de Ciencia de Materiales de Sevilla, C.S.I.C.-Universidad de Sevilla, C. Américo Vespucio nº49, 41092 Sevilla, Spain.

[2] Faculty of Physics, University of Seville, Avenida Reina Mercedes s/n, Sevilla, Spain.

[3] Departamento de Química Inorgánica, Facultad de Química, Universidad de Sevilla, Sevilla 41071, Spain.

[4] X-Ray Laboratory (CITIUS), University of Seville, Avenida, Reina Mercedes, 4B, Sevilla, Spain

Abstract

The multicycle CO_2 capture performance of CaO derived from the calcination of ball-milled limestone and dolomite have been tested under high temperature and high CO_2 concentration environment for the first time. Here it is shown that the CO_2 capture capacity of CaO is inversely related to the milling power applied to the starting mineral and the size of nascent CaO nanocrystals. In situ X-ray diffraction analysis used to follow the average crystallite size of $CaCO_3$ and CaO during the calcination process as a function of temperature demonstrates that crystal growth is notably enhanced in CO_2 rich atmosphere and milled sorbents. Contrary to early reports suggesting improved reactivity towards carbonation of CaO from milled sorbents, promoted agglomeration and crystal growth under this more "realistic" conditions lead to a severe deterioration of both capture capacity and recyclability as observed by the multicyclic carbonation/calcination experiments. Yet the negative effect of milling is less pronounced in dolomite due to the constrained sintering effect of the inert MgO grains that results in smaller CaO crystallite sizes, reduced crystal growth rate and improved performance. These results provide insight on the role of CaO crystallinity on the carbonation reaction, useful for devising strategies to improve sorbents performance.

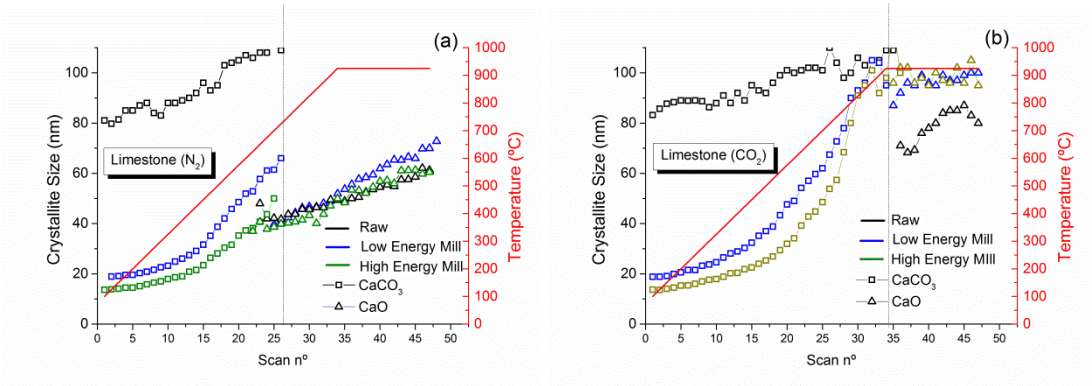

*Pedro E. Sánchez Jiménez
Instituto de Ciencia de Materiales de Sevilla,
C. Américo Vespucio nº49, 41092 Sevilla, Spain
Tel +34954489548 Fax +34954460665
e-mail address: pedro.enrique@icmse.csic.es

Influence of ball milling on CaO crystal growth during limestone and dolomite calcination: Effect on CO_2 capture at Calcium Looping conditions.

Pedro E. Sánchez-Jiménez[1,*], *José M. Valverde*[2], *Antonio Perejón*[1,3], *Antonio de la Calle*[1, 2], *Santiago Medina*[4] *and Luis A. Pérez-Maqueda*[1]

[1] Instituto de Ciencia de Materiales de Sevilla, C.S.I.C.-Universidad de Sevilla, C. Américo Vespucio nº49, 41092 Sevilla, Spain. [2] Faculty of Physics, University of Seville, Avenida Reina Mercedes s/n, Sevilla, Spain.

[3] Departamento de Química Inorgánica, Facultad de Química, Universidad de Sevilla, Sevilla 41071, Spain.

[4] X-Ray Laboratory (CITIUS), University of Seville, Avenida, Reina Mercedes, 4B, Sevilla, Spain

*Corresponding author: pedro.enrique@icmse.csic.es

Abstract

The multicycle CO_2 capture performance of CaO derived from the calcination of ball-milled limestone and dolomite have been tested under high temperature and high CO_2 concentration environment for the first time. "Here it is shown that the CO_2 capture capacity of CaO is inversely related to the milling power applied to the starting mineral and the size of nascent CaO nanocrystals. In situ X-ray diffraction analysis used to follow the average crystallite size of $CaCO_3$ and CaO during the calcination process as a function of temperature demonstrates that crystal growth is notably enhanced in CO_2 rich atmosphere and milled sorbents. Contrary to early reports suggesting improved reactivity towards carbonation of CaO from milled sorbents, promoted agglomeration and crystal growth under this more "realistic" conditions lead to a severe deterioration of both capture capacity and recyclability as observed by the multicyclic carbonation/calcination experiments. Yet the negative effect of milling is less pronounced in dolomite due to the constrained sintering effect of the inert MgO grains that results in smaller CaO crystallite sizes, reduced crystal growth rate and improved performance. These results provide insight on the role of CaO crystallinity on the carbonation reaction, useful for devising strategies to improve sorbents performance.

1. Introduction

The Calcium looping (CaL) process, based on the reversible carbonation reaction of CaO at high temperature with CO_2 to produce $CaCO_3$, has received considerable attention in the last years as a cost-effective technology for CO_2 capture from post-combustion emissions. Out of the numerous possible CaO precursors, natural limestone ($CaCO_3$) stands as the most promising one due to its low cost (<10$/ton), wide availability and non-toxicity [1]. In a typical CaL process, calcium oxide particles react in a fluidised gas-solid reactor with CO_2 from a post-combustion gas stream at temperatures around 650 ºC and CO_2 volume concentrations of about 15%. The newly formed $CaCO_3$ particles are then transferred into a calciner where calcium oxide is regenerated for reuse in a new carbonation/calcination loop. In order to produce a high purity CO_2 stream that can be retrieved for storage or other uses the calciner must be kept under high CO_2 partial pressure (typically ~70-90% CO_2 vol concentration at atmospheric pressure) [1-6]. Since the process is highly reversible, $CaCO_3$ decarbonation is strongly hindered by high concentrations of CO_2 in the calcination environment thereby high temperatures of about 950 ºC, well above the equilibrium temperature (around 900ºC), are needed for a complete decarbonation in short residence times [7-12]. Such high temperatures can be reached in practice by oxy-combustion, which imposes a severe penalty to the process due to fuel consumption and additional CO_2 production [4, 5, 13-19]. A further inconvenience of the CaL process is the rapid deterioration of the sorbent capture capacity over multiple carbonation/calcination cycles that makes unavoidable to periodically replace the spent sorbent with a new fresh s makeup. Limestone derived CaO (lime) deactivation is mostly caused by the sintering of nascent CaO particles during the $CaCO_3$/CaO transformation in the calciner through an oriented aggregation mechanism that leads to a reduction in both CaO surface area and porosity [2, 20-25]. Such process is aggravated by the high CO_2 partial pressure and high temperatures in the calcination environment, which enhance CaO nanocrystals aggregation and sintering therefore significantly promoting sorbent deactivation [11, 15, 22-24, 26]. Another parameter with a significant role on sorbents performance is the presence of water vapour. The combustion flue gas contains about a 5-15% vol. concentration of steam. It is know that water plays a role as mass transport heat transfer medium as well as recrystallization agent [22, 27-30].

As overcoming these handicaps is key for a competitive deployment of the CaL process at the industrial level [2, 12, 31], a great effort has been devoted in the last years to improve the current fundamental understanding of the calcination/carbonation reactions and the physicochemical background underlying sorbent deactivation, which is not completely understood yet [11, 20, 22, 23, 26, 32-41]. The most widely explored approaches to mitigate sorbent deactivation and to enhance the CO_2 capture performance are thermal pretreatments for prolonged periods [42-48] and the use of nanostructured inert additives that constrain aggregation and sintering of the incipient calcium oxide

nanocrystals [36, 39, 49-59]. Despite early evidences of sorbent self-reactivation after prolonged thermal pretreatments carried out in air [43, 44], it was later found that any reactivation effect was effectively suppressed when calcination in the CaL cycles was implemented under high CO_2 partial pressure as necessarily required in practice [23]. Only when a brief recarbonation phase is introduced in between carbonation and calcination stages, the overall performance of thermally pretreated lime is seen to improve significantly although in that case a further reactor for recarbonation would be needed [47].

Recent works have revealed that the effect of thermal treatment and additives might be related to sorbent crystallinity and reaction kinetics. Thus, defects and lattice stresses in low crystalline sorbents would promote solid state diffusion hence enhancing both carbonation and decarbonation kinetics whereas the highly crystalline sorbents seem to exhibit a comparatively poor reactivity [26, 35, 60-62]. Therefore, annealing at high temperatures during long times would promote the aggregation and growth of crystals and severely hamper recarbonation [35, 62]. The presence of water in the calciner environment also affects the crystallinity of the sorbents. Thus, it has been reported that water catalyses CaO sintering thereby resulting in a decrease of the surface area due to crystallite growth and pore closure [22]. On the other hand, some authors have recently observed that steam reactivates spent sorbent [28] , enhances reactivity [29] and induces the formation of a stable pore structure that minimizes the decay in the sorbent carrying capacity [29, 30] The presence of superheated steam is also known to accelerate the calcination reaction albeit it also promotes CaO friability[63, 64].

The sorbent inactivation can also be reduced by the inclusion of inert additives, as naturally occurs in the case of dolomite, ($CaMg(CO_3)_2$), which has been proposed as an alternative to limestone CaO precursor. Besides being widely available and cheap, CaO derived from dolomite calcination (dolime) also exhibits consistently higher CO_2 capture capacity and attenuated sorbent deactivation in comparison to lime at high temperature and high CO_2 partial pressure conditions [26, 61, 65-67]. On heating, dolomite decomposes directly into MgO and CaO at temperatures around 700 ºC. As recently shown using in-situ X-Ray diffraction analysis coupled to thermogravimetric (TG) studies of calcination under a CO_2 enriched environment the just formed CaO instantly recarbonates [26, 68-70] into fresh, low crystalline $CaCO_3$ that afterwards decomposes at a higher temperature as determined by the thermodynamic equilibrium, yielding a poorly crystalline and therefore highly reactive CaO [11, 26]. Moreover, the inert MgO grains formed as a result of dolomite calcination conform a skeleton over which the $CaCO_3$/CaO layer builds up and breaks down along the ensuing carbonation/calcination cycles thus hindering the growth of CaO nanocrystals [61, 71]. The net result produced by the constrained sintering effect granted by the the inactive MgO frame and the enhanced decarbonation kinetics of the nanocrystalline $CaCO_3$ is a significant decrease in the minimum temperature required for attaining full decarbonation in short residence times. As a beneficial side effect, the reduced temperature also mitigates sorbent deactivation [61, 72]. Consequently, dolomite exhibits both higher capture capacities from the first cycle and attenuated deactivation. Nevertheless,

after a number of successive carbonation/calcination cycles the MgO grains segregate progressively from the CaO and their stabilizing effect fades out [72].

All things considered, the most effective way to inhibit CaO sintering; and therefore mitigate sorbent deactivation, appears to be lowering down the effective calcination temperature. Thus, it may be envisaged that enhancing decarbonation kinetics via crystallinity reduction is a feasible method to achieve the desired temperature reduction. The simplest and most practical method for reducing the crystallinity of solids is mechanical grinding [73, 74]. However, except for a few works, the CaL behaviour of milled sorbents has not been analyzed in detail [35, 62, 75]. In those studies, the behaviour of milled and annealed sorbents suggests that the strain and high defect concentration of milled $CaCO_3$ would favour diffusion in the carbonation stage eventually leading to higher CaO conversions and faster reaction kinetics [35, 62]. Nevertheless, the tests presented in those works were not performed under the harsh calcinations conditions of high temperature and high CO_2 partial pressures in the calciner required in CaL plants. Thus, it is of paramount importance to study whether the beneficial effect of mechanical grinding of natural minerals on the CO_2 capture capacity of the sorbents is maintained when calcination is carried out under these harsher conditions. Mechanical grinding would be a cost-effective treatment to reduce the calcination temperature and, consequently, mitigate the energy penalty of the process in order to ensure the industrial competitiveness of the CaL technology. Here, we study the CO_2 capture performance under high temperatures and in a high CO_2 partial pressure environment of both limestone and dolomite samples previously subjected to mechanical grinding by ball milling. The effects of milling on particle size, microstructure and crystallinity of limestone and dolomite as well as on their multicycle calcination/carbonation behaviour have been analyzed in detail.

2. Experimental

The results here presented have been obtained using natural limestone (99.6% $CaCO_3$) retrieved from Matagallar quarry (Pedrera, Spain) and natural dolomite from Bueres (Spain). The average particle size of limestone is 4.6 μm whereas dolomite was sieved to keep the particle size under 45 μm to prevent decrepitation phenomena during thermal decomposition.[76].

Limestone and dolomite samples were mechanically grinded using two different mills, which provided different milling energy levels. A gentler treatment was performed using a Fritsch Pulverisette 6 centrifugal mill (Idar-Oberstein, Germany) in which the milling media consisted of a 100 cm^3 steel jar and 200 tungsten carbide balls with a diameter of 5.5 mm. Weight to ball ratio was set at 1:40. The materials were milled for 2 hours at 500 r.p.m. Alternatively, highly energetic milling treatments were carried out using a SPEX 8000M mixer/mill where milling was carried out

using 20 cm^3 steel jar with 5 balls of 12 mm diameter. In this case the weight to mass ratio was set to 1:20. This energetic grinding was applied also for 2 hours.

In-situ XRD analysis during calcinations has been carried out using a powder diffractometer (Bruker D8 Advance) equipped with a high temperature chamber (Anton Paar XRK 900) and a fast response/high sensitivity detector (Bruker Vantec 1). The full description of the experimental set-up can be found in a previous publication [26]. Temperature during in situ XRD experiments was raised at 10 °C min^{-1} up to 925 °C. XRD scans of 295 s were recorded in the range of $20° < 2\theta < 60°$ (0.03° per step). each 25 °C starting at 400 °C. Once a temperature of 925 °C is reached, the temperature is maintained for 1 hour while XRD scans are continuously recorded for 1 h. Scans were all registered at constant temperature.

The multicycle CO_2 capture behaviour of the different sorbents was studied using a Q5000IR (TA instruments)thermogravimetric instrument . This instrument is equipped with a furnace heated by halogen lamps that allows for high heating/cooling rates up to 300 ºC/. That allows to achieve very fast transitions between the consecutive carbonation/calcinations (carb/calc) stages programmed at different temperatures, thereby preventing any transformations to occur during the ramps as would occur in conventional furnaces. Fast transitions between the carbonation and calcination phases are especially important not only to mimic as close as possible the situation in a CaL plant but it also served to prevent the significant recarbonation that would happen if the partially carbonated sorbent were slowly heated up in high concentration of CO_2, as it has been previously observed [42]. Small sample size of about 10 mg were employed in order to minimize heat and mass transfer phenomena as it would occur in fluidized bed (CFB) reactors[77], as well as intra-particle diffusion resistance [9].

Particle size distributions (PSD) were determined by means of a Mastersizer 2000 (Malvern Instruments Ltd.) instrument. The samples were dispersed in 2-propanol and sonicated for 5 seconds to break up aggregates with the goal of assessing the mechanical stability of the sorbents as affected by the CaL cycles. Particle friability as caused by thermal stresses may affect adversely the performance of the CaL process by a substantial loss of fine particles that cannot be captured by conventional cyclones [2, 78].

3. Results and discussion

3.1 Effect of mechanical grinding on limestone and dolomite microstructure.

In order to assess the influence of milling energy on the microstructure of limestone and dolomite, two different mills were employed; a centrifugal mill, which imposes a relatively mild treatment to

the sorbent, with an important contribution of shear over impact [74], and a SPEX shaker mill, in which the specimen cup moves in a 8-like figure pattern, providing a high amount of energy to the sorbent through the impact of the grinding media. Regardless of the mill employed, all materials were grinded for 2 hours. The series of XRD diffractograms illustrated in Figure 1 shows a significant amorphization undergone by the natural minerals as a consequence of grinding, which is expectedly more intense in samples mechanically treated in the highly energetic SPEX mill. Limestone mostly consists of pure calcite, whereas the XRD pattern of dolomite shows also the presence by a small amount of calcite impurities. Crystallite size of the different materials can be roughly estimated from the peak broadening using Scherrer`s method. The resulting values are plotted in Figure 2, showing that the initial $CaMg(CO_3)_2$ and $CaCO_3$ are composed of large crystals, with coherent domain lengths well over 100 nm, which is approximately the upper limit that can be confidently estimated by Scherrer's equation. As inferred from Figure 2 even a mild milling treatment greatly reduces crystallite size to values slightly over 20 nm, with the more energetic treatment further reducing the coherent crystal length to about 15 nm. No significant differences are seen in the effect produced upon either dolomite or limestone.

Figure 3 shows the particle size distributions (PSD) of both unmilled and milled materials. It can be noticed that the mechanical treatment does not yield particles smaller than those already present in the starting material although the population of fine particles is notably increased. Milling leads however to an increase of the average particle size due to the formation of large particles because of cold welding as generally observed for milled powders [74]. Thus, the initial volume weighted mean particle size of limestone increases from 4.6 μm up to 20 μm and 30 μm for the samples grinded in the centrifugal and SPEX mills, respectively. As occurred for limestone, for milled dolomite particles smaller than the initial ones are not formed, albeit there is a significant increase in the population of particles under 10 μm due to fragmentation of larger particles. Also, dolomite milled in the SPEX contains a small number of very large particles probably formed by cold welding. The volume weighted mean particle size observed after treatment in the centrifugal and SPEX mills are 30 μm and 60 μm respectively. Volume weighted mean particle size values are plotted in Figure 2, which illustrates that the net effect of the mechanical treatment is a reduction in the crystallite size accompanied by an increase of particle size due to cold welding. Figure 4 shows SEM micrographs of limestone and dolomite, before and after mechanical treatment that illustrate the described effect of milling on particle size. Moreover, EDS analysis of milled dolomite samples (Figure S1 in the Supplementary Information) indicates a homogeneous distribution of calcium and magnesium all over the sample. This important observation dismisses the possibility, previously suggested by other authors, of an eventual segregation of $MgCO_3$ and $CaCO_3$ as a result of the mechanical treatment [79-81], which would presumably explain the occurrence of half-decomposition at reduced temperatures during calcination as will be seen also in our work.

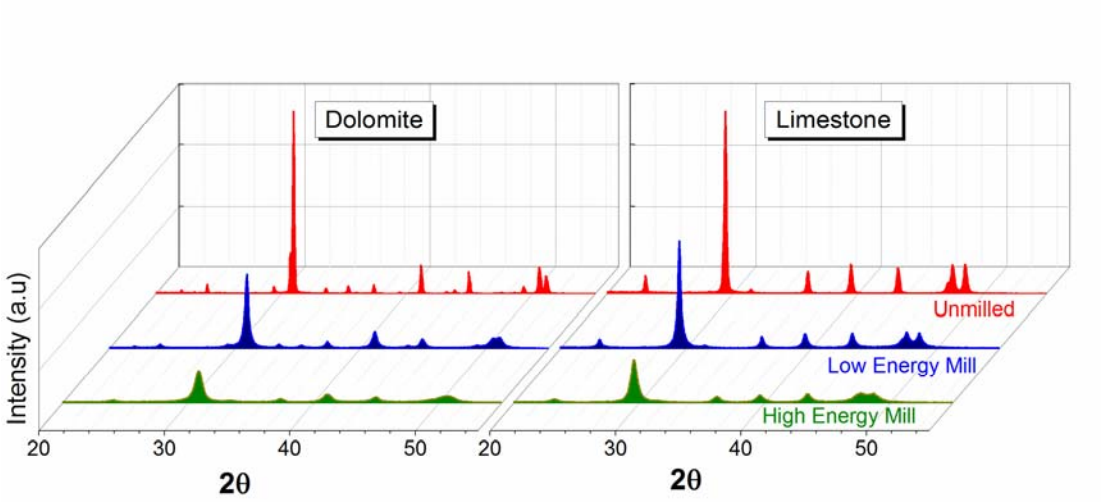

Figure 1. XRD diffractograms obtained for raw (unmilled) dolomite and limestone and milled samples at different milling energy intensities.

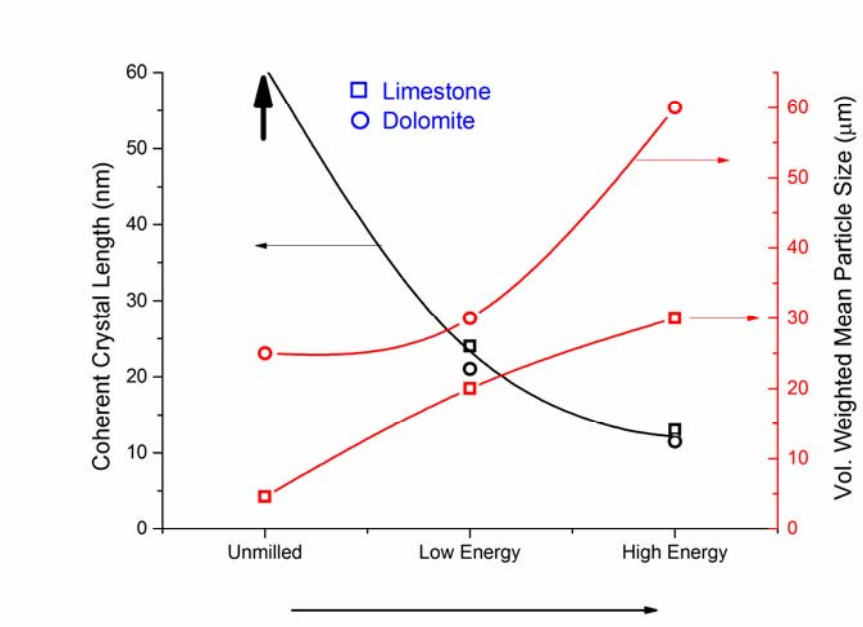

Figure 2. Coherent crystal domain length and volume weighted mean particle size measured for both milled (at different energy intensities) and unmilled limestone (squares) and dolomite (circles) obtained from XRD and PSD analysis, respectively.

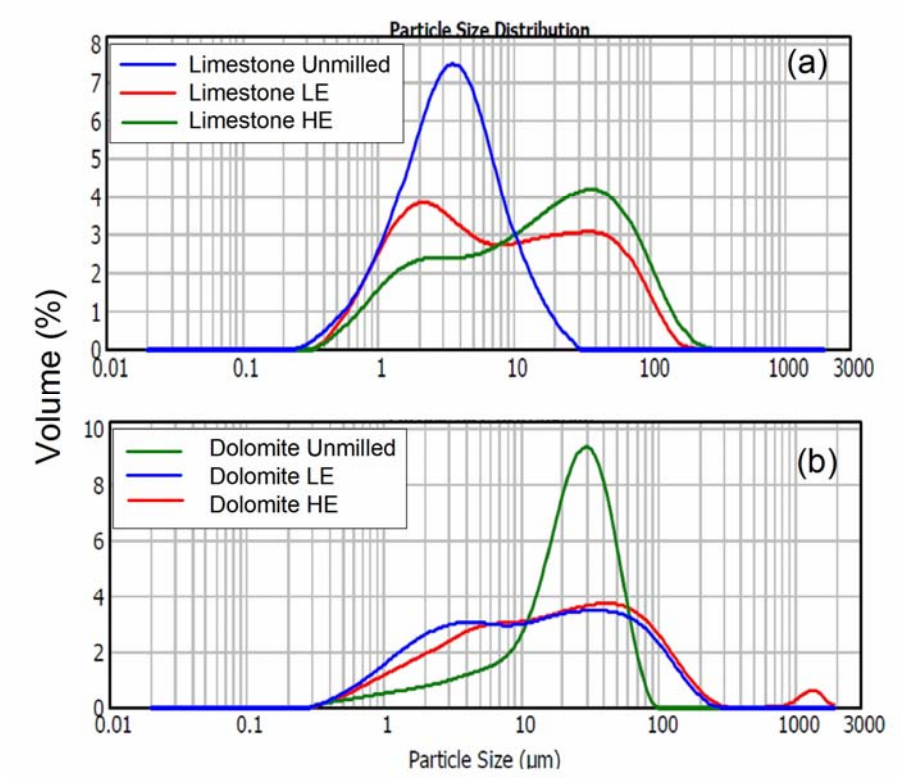

Figure 3. Particle size distributions (PSD) obtained for unmilled and milled (a) limestone and (b) dolomite samples under different milling energy intensities.

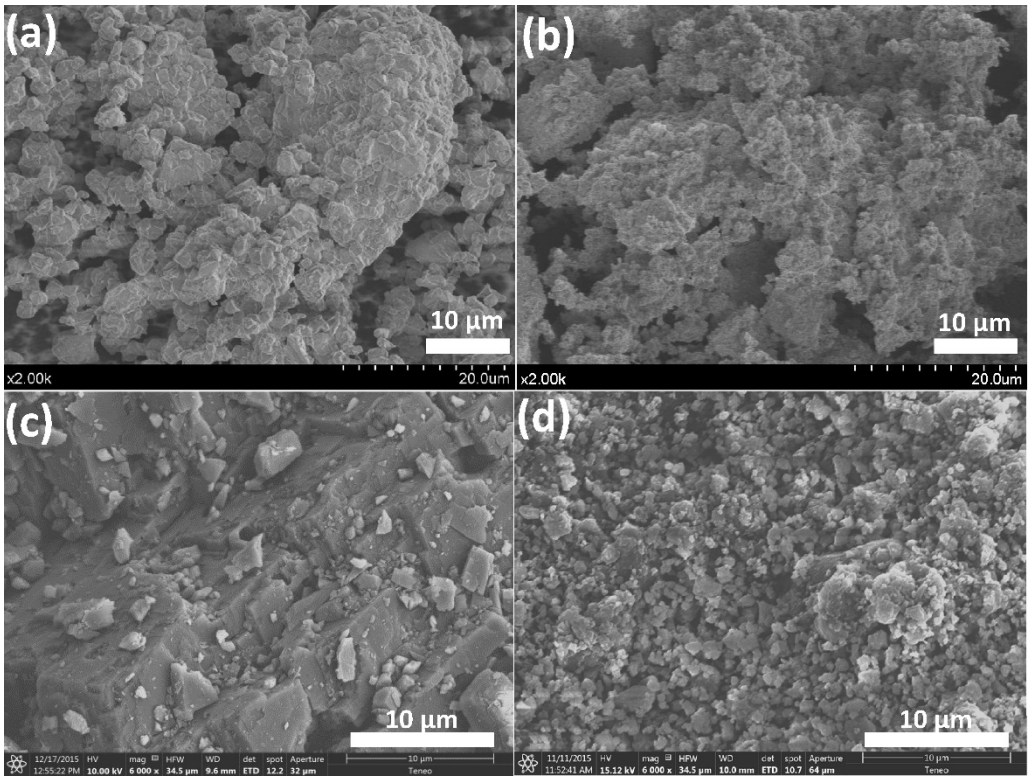

Figure 4. SEM micrographs corresponding to (a) unmilled limestone, (b) limestone after 2 hours of centrifugal milling, (c) dolomite and (d)) dolomite after 2 hours of centrifugal milling.

3.2 Effect of mechanical grinding on the multicycle CO_2 capture performance of limestone and dolomite.

The carbonation/calcination loops were recorded according to the following schedule; (i) an initial pre-calcination from room temperature up to 900 ºC at 300 ºC/min in 70% CO_2 / 30% air (vol/vol), (ii) 5 minutes long carbonation stages at 650 ºC in a 15% CO_2 / 85% air (vol/vol) atmosphere and (iii) 5 minutes long calcination stages at 900 ºC in 70% CO_2 / 30% air (vol/vol) atmosphere. Temperature shifts between carbonation and calcination stages were carried out at 300 ºC/min to replicate as closely as possible the fast transitions required in a practical application. Sorbent regeneration temperature of 900 ºC is somewhat lower than the temperature typically needed (~930-950ºC) in pilot-scale plants to attain full calcination of limestone in short residence times. That value of temperature has been selected since previous studies have proven that full calcination of dolomite

derived CaO is perfectly feasible at such relatively low temperatures [61]. Moreover, as will be seen below, mechanical milling serves to enhance decarbonation at reduced temperatures.

Figure 5 illustrates the changes in weight % with the temperature during the pre-calcination and the ensuing carbonation/calcination cycles for raw and milled limestone. The same plots are shown in Figure 6 for raw and milled dolomite. As can be seen, experimental results in Figure 5 indicate that complete decarbonation of fresh limestone cannot be fully attained during precalcination in a 70% vol. CO_2 concentration atmosphere at 900 ºC. Several carb/calc cycles are needed before CaO can be completely regenerated in a 5-minute long calcination step. This is due to the high reversibility of $CaCO_3$ decomposition into CaO and CO_2 so that the presence of CO_2 at high concentration in the calcination environment severely hinders the forward reaction [7-11]. Thus, temperatures well over the equilibrium temperature are needed to achieve complete decarbonation in short residence times. Moreover, the highly crystalline $CaCO_3$ in raw limestone is characterized by a low decarbonation rate so that complete regeneration of CaO is only possible once the repeating carb/calc cycles eventually erase the memory of the initial structure and progressively decrease $CaCO_3$ crystallinity [35]. On the other hand, it may be seen that the previously ball-milled limestone does attain full decarbonation during the initial heating ramp up to 900ºC (Figure 5). Arguably, the highly disordered microstructure of the milled sorbent, composed of crystallites about 5 times smaller than in raw limestone, helps full decarbonation from the very first cycle. However, faster decarbonation kinetics leads also to a noticeably lower capture capacity along the following cycles as inferred from Figure 5b and 5c.

Figure 6 shows that, in contrast to limestone, the nascent $CaCO_3$ derived from half-decomposition of raw dolomite is fully decarbonated and recarbonated in short times from the 1st carb/calc loop using a calcination temperature of 900 ºC, as previously reported [72]. Interestingly, the effect of mechanical treatment on the initial decarbonation of dolomite appears opposite to that observed in limestone. Thus, grinding in the more energetic SPEX mill hinders decarbonation so that about three carb/calc loops are needed to achieve full CaO regeneration in the 5-minute calcination stage. As in the case of limestone, it can be seen that milling is detrimental to the overall capture capacity performance of the dolomite derived sorbent in subsequent carb/cal cycles.

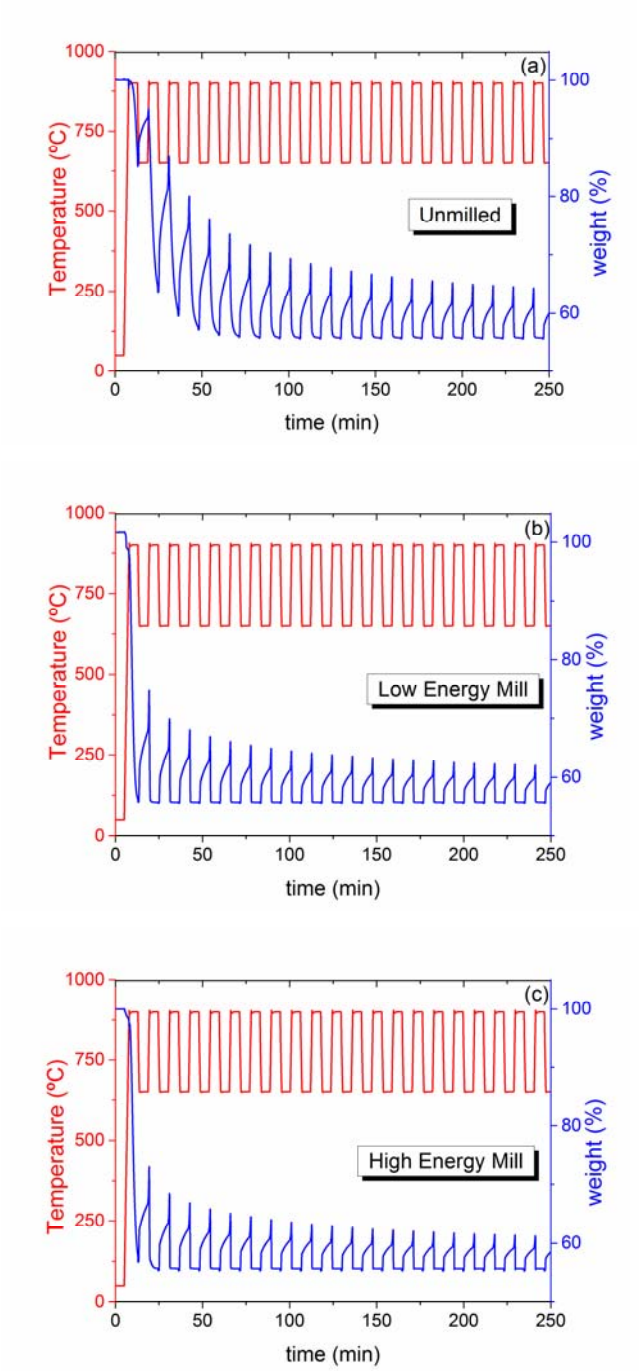

Figure 5. Multicycle carb/calc behaviour of limestone, (a) fresh unmilled sample, (b) sample subjected to low energy milling and (c) sample subjected to high energy milling. Carbonations were carried out at 650 ºC in 15% CO_2 / 85% air (vol/vol) for 5 min and calcinations at 900 ºC in 70% CO_2 / 30% air (vol/vol) for 5 min.

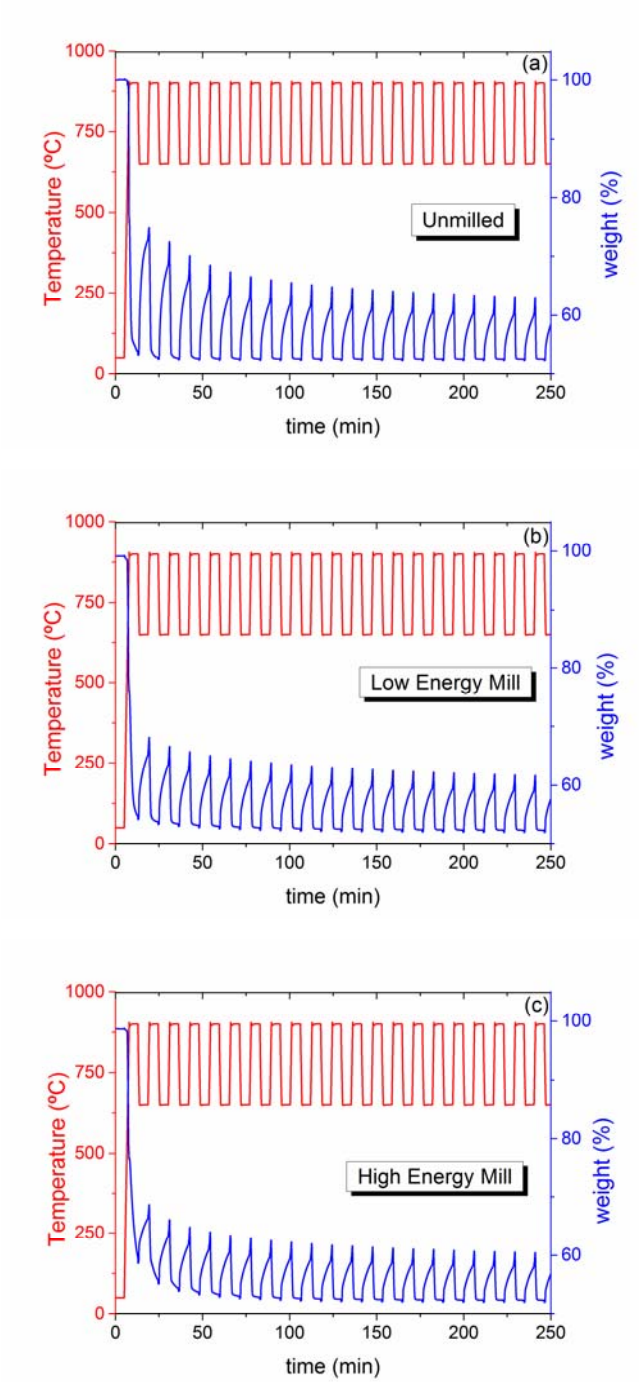

Figure 6. Multicycle carb/calc behaviour of dolomite, (a) fresh unmilled sample, (b) sample subjected to low energy milling and (c) smple subjected to high energy milling. Carbonations were carried out at 650 ºC in 15% CO_2 / 85% air (vol/vol) for 5 min and calcinations at 900 ºC in 70% CO_2 / 30% air (vol/vol) for 5 min.

CaO conversion, X_N, which is defined as the ratio of CaO mass converted to $CaCO_3$ to the CaO mass before carbonation, is a parameter often employed for process simulations and economic analysis on the integration of the Calcium Looping technology into fuel thermal plants [3, 19, 82] In general, X_N displays a decay trend along a number of cycles that can normally be described by the following semi-empirical fitting equation [24, 83]:

$$X_N = X_r + \frac{X_1}{k(N-1) + (1 - X_r/X_1)^{-1}}; \quad (N = 1,2,\dots) \quad (1)$$

where N is the cycle number, X_1 is CaO conversion in the first cycle, k is the deactivation constant and X_r the residual conversion. Previous works have reported that limestone yields a residual conversion of about 0.07-0.08 and a deactivation constant k close to 0.5 [24, 34]. The evolution of X_N with the cycle number for all the sorbents analysed is shown in Figure 7, together with the best fit curves of Eq (1) to experimental data. Residual conversion and deactivation constant values are summarized in Table 1. As may be observed, mechanical grinding of the sorbent precursor results in severe hampering of conversion, even when mild centrifugal mills are employed. The reduction in conversion is also directly related to the milling power employed. An additional conclusion can be drawn from the analysis; residual conversion of dolomitic CaO is about three times that of lime for the same conditions. Besides, although milling does not have a significant influence on the residual conversion of limestone, which is already quite low in the raw mineral, it does reduce dolomite derived CaO conversion along the entire loop range, as was previously hinted from the cycles shown in Figure 2. Thus, our work shows that the harsh calcination conditions of high temperature and high CO_2 partial pressure, which are necessarily involved in "realistic" CaL looping processes for CO_2 capture, actually reverse the potentially beneficial effect that mechanical grinding had on the sorbents performance previously reported in milder calcinations conditions [62, 75]. As inferred from the results here presented the mechanical treatment of the sorbents hinders both the decarbonation of dolomite derived $CaCO_3$ and the subsequent recarbonation of the regenerated CaO. Deterioration of the sorbent capture capacity is more marked when higher milling power is used, which suggests that milling would favour MgO/CaO segregation by diffusion at high temperatures. In spite of that, dolomite displays larger CaO conversion values than limestone, which can be explained by the stabilizing effect granted by the MgO particles as previously reported [61, 72].

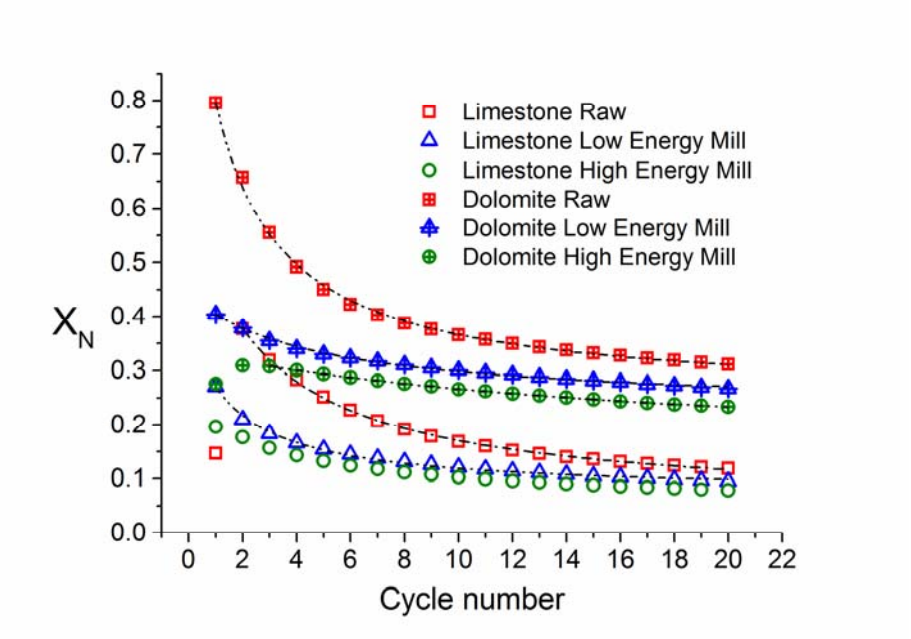

Figure 7. CaO conversion X_N versus cycle number obtained for limestone and dolomite. The lines are best fit curves from Eq. (1) to the data.

TABLE 1. Deactivation constant *k*, residual conversión X_r and correlation coefficient r^2 obtained from the best fits of Eq (1) to experimental data (Figure 7)

CaO precursor	Pretreatment	X_r	k	r^2
Limestone	Raw	0.049 ± 0.002	0.245 ± 0.005	0.999
	Low energy mill	0.074 ± 0.002	0.520 ± 0.030	0.996
	High energy mill	0.076 ± 0.002	0.228 ± 0.006	0.999
Dolomite	Raw	0.247 ± 0.004	0.581 ± 0.021	0.998
	Low energy mill	0.230 ± 0.003	0.410 ± 0.030	0.999
	High energy mill	0.139 ± 0.001	0.086 ± 0.002	0.999

3.3 Influence of material crystallinity on CaO conversion

Recent works have highlighted the important role of the crystal structure of the sorbent precursor on both CaO carbonation and $CaCO_3$ decarbonation reactions [11, 26, 32, 60, 62]. On the other hand, carbonation of calcium oxide particles occurs along two well differentiated stages; a fast reaction-controlled (FR) stage due to the chemical reaction of the CO_2 molecules on the surface of CaO grains followed by a much slower solid state diffusion (SD) stage driven by the counter-diffusion of CO_3^{2-} and O^{2-} ions across the barrier carbonate layer formed in the previous stage [84-89]. In previous studies, it has been reported that grinded limestone exhibits higher conversion values in the few first cycles at the expense of larger deactivation rates when CaO is produced by calcination of $CaCO_3$ under low CO_2 partial pressure [60]. Those studies showed that whereas conversion of milled samples during the FR stage seemed to be largely unaffected, the reaction kinetics of the SD stage was significantly enhanced since the reduced crystallinity and higher density of structural defects would promote the counter-diffusion of CO_3^{2-} and O^{2-} ions responsible of the diffusive driven carbonation [35, 60, 90]. Yet, enhanced lattice diffusion of nanosized crystals accelerates also the sintering of the CaO particles during the calcination stages thereby reducing the available specific surface area of the CaO skeleton over which the carb/calc cycles builds up and leading to an irreversible loss of CaO conversion [35, 60]. On the other hand, sorbents subjected to a prolonged heating treatment previously to the carb/calc looping usually exhibit lower initial conversions in the first cycle due to the marked sintering of the produced CaO particles during thermal pretreatment, albeit with a notably reduced deactivation [60].

In a similar way, decarbonation kinetics is also strongly influenced by crystallinity. Thus, thermal annealing in a CO_2 rich atmosphere at temperatures close but below the equilibrium temperature serves to increase the size of the $CaCO_3$ calcite crystals in limestone by reducing the density of dislocations and defects [20, 35, 91]. Moreover, in-situ XRD analyses have shown that the crystallite size of nascent CaO formed during the decomposition of $CaCO_3$ in the presence of CO_2 were larger the higher the CO_2 partial pressure in the environment [11, 26]. Several works have reported the increased resistance of a thermally annealed sample to diffusion [92, 93]. As a consequence, under high temperature and high CO_2 partial pressure, such highly crystalline limestone exhibits a rather slow decarbonation rate.

The multicycle capture behaviour of unmilled natural limestone shown in Figure 5 is consistent with previously reported results. At a temperature of 900 ºC the decarbonation process takes place at a rate so slow that full calcination is not fully achieved after the first few 5-min calcination stage. Nevertheless, since each recarbonation of the calcite derived CaO entails a reduction in crystallinity with respect to the starting material [35, 89], after a few loops the decarbonation kinetics of the freshly formed $CaCO_3$ eventually becomes fast enough to attain full conversion into CaO at 900ºC in short residence times. On the other hand, ball-milled limestone, composed of heavily strained small calcite

crystals, exhibits sufficiently fast decarbonation kinetics to complete the conversion into CaO just after the first initial calcination at 900 ºC. Nevertheless, decarbonation is speeded up at the expense of a severe deterioration in the capture capacity along the cycles.

Figure 8 shows a detail of the 10th and 20th carb/calc, where the FR and SD carbonation regimes are readily apparent. As can be seen, carbonation in the SD regime is a main contributor to the overall carbonation in the 5 min period of our experiments. It can be inferred also that both the FR and SD driven carbonation stages in milled limestone are hindered albeit decarbonation of the $CaCO_3$ formed is fastened. Also, the deactivation rate appears much higher for unmilled limestone as the initial diffusive carbonation rates of unmilled and milled limestone become similar with the number of cycles. This behaviour is quite the opposite of what has been reported so far for calcinations carried out under low CO_2 partial pressure [35, 62, 75]. The rate of diffusive carbonation is governed by crystal structure [35, 62]. Thus, the most plausible explanation for this behavior is that the enhanced sintering that $CaCO_3$ normally undergoes in a CO_2 rich atmosphere is additionally enhanced in the highly reactive milled $CaCO_3$. Thus, precalcination of the milled samples entails a severe sintering as well as a reduction of structural defects that hampers capture capacity in the subsequent cycles especially in the SD driven stage. As can be observed in Figure 8, the carbonation rate of the unmilled limestone slowly approaches that of the milled limestone, as the repeated carb/calc loops slowly take the initially less sintered unmilled $CaCO_3$ to the same level of sintering of the milled sorbent.

The detail of the 10th and 20th carb/calc cycles in Figure 8b illustrates also a different behaviour for dolomite as compared to limestone. Like in limestone, increasing the milling energy entails a reduced carbonation capacity. However, such reduction is less intense since dolomitic CaO is more resistant to deactivation by sintering presumably due to the inert MgO particles that hinder the aggregation of the nascent nanocrystals. Thus, the sorbent retains a more porous structure resulting in higher proportion of CaO after $CaCO_3$ decarbonation readily available conversion [61, 65, 66, 72]. Most of the decrease in capture capacity for milled dolomite is again mostly due to a lower carbonation rate during the SD driven stage. FR carbonation occurs at approximately the same rate and up to the same level of uptake for the three samples. Nevertheless, in contrast to limestone, the decrease in the reaction rate with the cycle number appears similar in all three samples and therefore independent of the mechanical pretreatment. Finally, the decarbonation rate appears to be mostly unaffected by the milling treatment and remains approximately the same regardless of the milling intensity. In order to dismiss any possible effect of the formation of large particles by milling on the multicycle CO_2 capture behaviour, CaL cycles were carried out in our work for sieved milled samples. The results (see Fig. S7 in Supplementary Information) did not reveal any influence that might arise from cold welding due to milling.

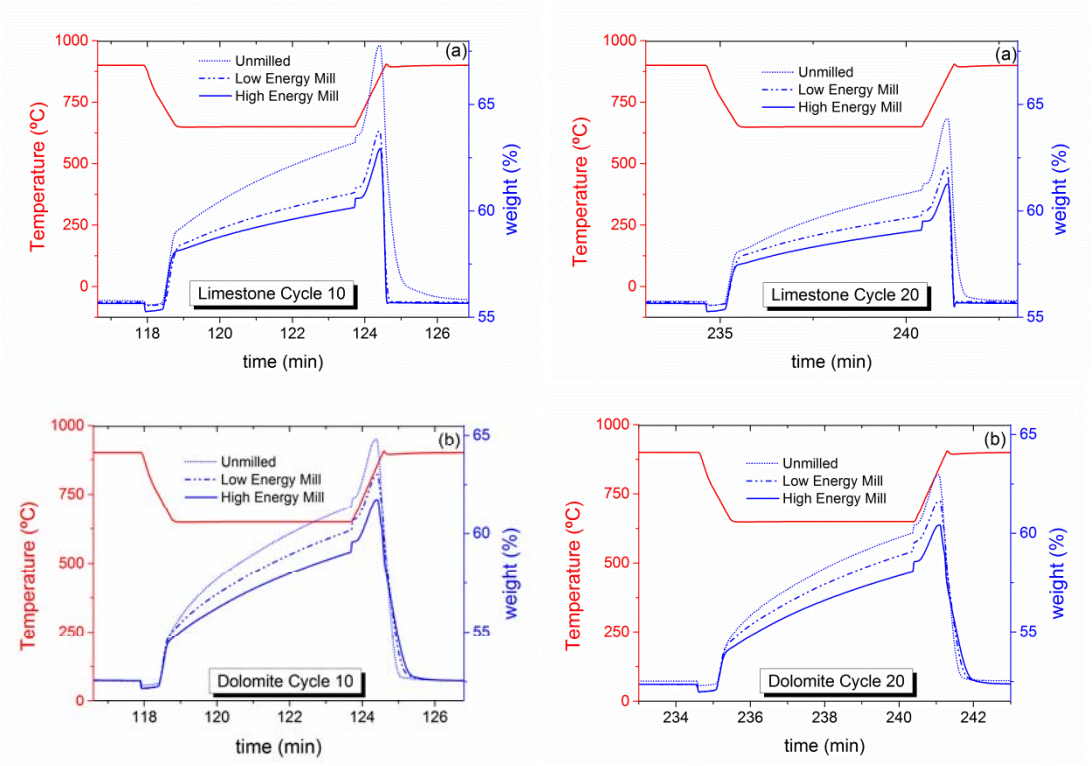

Figura 8. Thermograms obtained for the 10th and 20th carb/calc cycle of (a) limestone and (b) dolomite samples after different milling treatments.

3.4 In-situ XRD analysis

In order to get a grip on the influence of mechanical treatment and the calcination atmosphere on the sorbent precursor crystallinity, in-situ XRD measurements for calcination of the materials tested were carried out in a high temperature reaction chamber. Experiments were performed both in inert N_2 and reactive CO_2 to substantiate the reported influence of CO_2 in CaO and $CaCO_3$ crystal growth [22, 26]. Calcination was carried out in these tests by linearly increasing the temperature (10ºC/min) up to 925ºC, which was held constant afterwards for about 1 hour whereas XRD patterns were continuously recorded. Figure 9 and 10 show, as an example, a waterfall view of the XRD patterns obtained for the calcinations, in both N_2 and CO_2 atmosphere, of limestone and dolomite respectively grinded in a centrifugal mill. XRD diagrams for all studied samples can be found in the Supplementary Information (Figures S2 to S5). Figures 9a and 9b indicate that the main effect the CO_2 atmosphere has on calcite decarbonation is to delay the process to higher temperatures, as required by the thermodynamic equilibrium. On the other hand, the presence of CO_2 in the calcination environment during dolomite decomposition yields a qualitatively distinct behaviour

(Figures 10a and 10b). The XRD diagrams show how the starting $CaMg(CO_3)_2$ reflections in unmilled dolomite abruptly disappear at about 700 ºC, when it decomposes giving rise to nanocrystalline MgO and $CaCO_3$ which in turn decarbonates to yield CaO at about 925 ºC. Milled dolomite half-decomposition is hastened to temperatures as low as 600 ºC in agreement with previous observations [61, 69, 94]. Nevertheless, the conversion of $CaMg(CO_3)_2$ into MgO and $CaCO_3$ does not occur abruptly as in unmilled dolomite and both the decomposing dolomite and its products coexist during a temperature range comprised from 600 ºC to 700 ºC. This might be attributed to structural degradation and large lattice strains in grinded dolomite [95] as well as the wider distribution of particle sizes that not only promotes decomposition but also results in inhomogeneous reaction rates. Likewise, the subsequent decarbonation of the nascent $CaCO_3$ nanocrystals formed after milled dolomite half-decomposition also occurs along longer time periods. Thus, whereas $CaCO_3$ decarbonation starts in all three cases at about 925 ºC, in previously milled sorbents there are still significant amounts of $CaCO_3$ remaining even after 1- hour lag at 925 ºC. Finally, it is interesting to point out that dolomite decomposition in N_2 still produces a small amount of $CaCO_3$ together with the main products MgO and CaO. This is probably due to higher reactivity of nascent CaO, which immediately reacts with the CO_2 released after $CaMg(CO_3)_2$ half-decomposition. Thermal decomposition of dolomite is influenced by mechanical pretreatment as can be observed in TGA measurements. As seen in Figure 11, where the thermal decomposition of milled and unmilled dolomite as well as limestone are compared in 70% vol CO_2 using a heating rate of 10 ºC min^{-1}, $CaCO_3$ decomposition is shifted to higher temperatures due to the effect of CO_2 on reaction equilibrium. Also, dolomite half-decomposition is hastened and occurs during a wider temperature range.

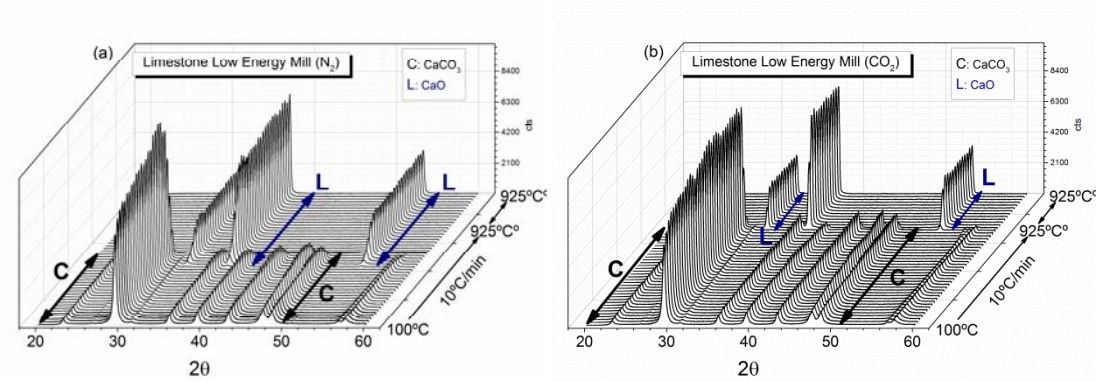

Figura 9. XRD scans obtained during in situ calcination of milled limestone under pure N2 (a) and CO2 (b). The main Bragg peaks of calcite (CaCO3) and lime (CaO) are indicated.

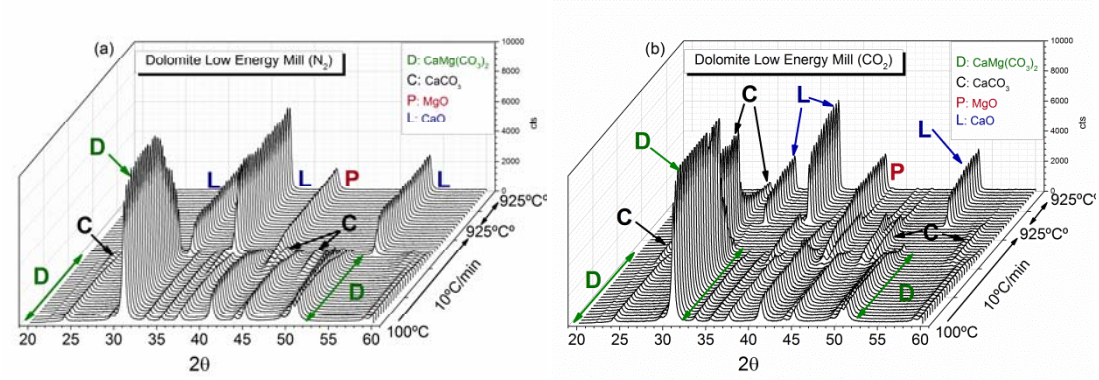

Figura 10. XRD scans obtained during in situ calcination of milled dolomite under pure N_2 (a) and CO_2 (b). Main Bragg peaks of dolomite ($CaMg(CO_3)_2$), calcite ($CaCO_3$), lime (CaO), and periclase (MgO) are indicated.

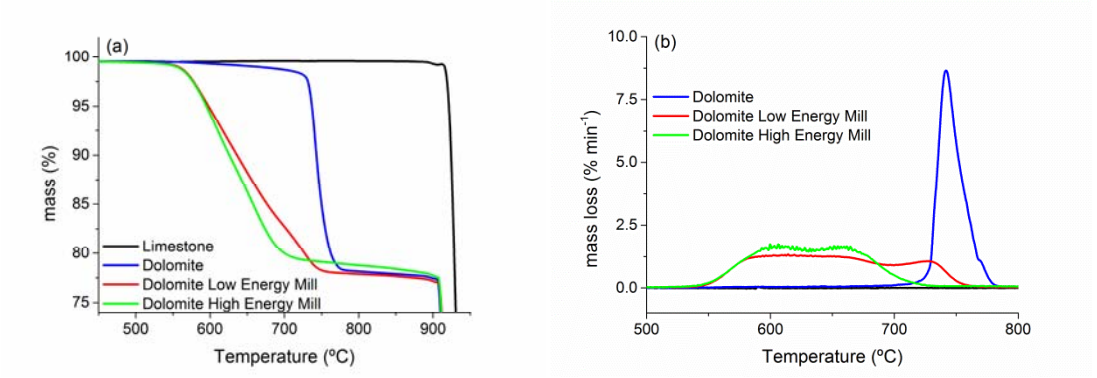

Figura 11. Thermograms obtained for the decomposition of limestone, dolomite and milled dolomite. (a) Mass vs temperature curves and (b) detail of the rate of mass loss vs. temperature during dolomite half-decomposition.

Nevertheless, in-situ XRD analysis allows us to obtain the coherent crystal length of the formed CaO, which is indicative of its reactivity towards carbonation as shown in previous works [72]. The coherent crystal length (crystallite size) of the different compounds involved in the calcination reaction was calculated by means of the Lebail quantitative method. Figure 12a shows the evolution with temperature of $CaCO_3$ and CaO crystallite sizes during limestone decomposition in N_2. As can be seen, both the crystallite size of nascent CaO and the growth rate of CaO crystals are independent of the mechanical treatment to which the raw limestone is subjected. On the other hand, as inferred from Figure 12b, the crystallite size of the nascent CaO is remarkable larger when calcination is performed under CO_2. Moreover, the coherent domain size of the CaO crystals formed from milled $CaCO_3$ appear notably larger than those produced from unmilled $CaCO_3$, which can be explained by the higher tendency to aggregate and sinter of the milled particles, as a consequence of both the higher number of grain boundaries in a sorbent composed of small crystallites and the effect CO_2 atmosphere, which greatly promote grain boundary diffusion [22, 23, 96] These results serve to rationalize the above observed detrimental effect of milling on the capture capacity of the derived CaO (as shown in Figure 8) since larger CaO crystals are less reactive towards carbonation [26, 72]. Regarding $CaCO_3$, mechanical milling leads to a nanocrystalline $CaCO_3$ structure with initial coherent crystal length of about 20 nm, but prone to sintering especially in the presence of CO_2 in the calcination environment as may be seen in Fig 13b.

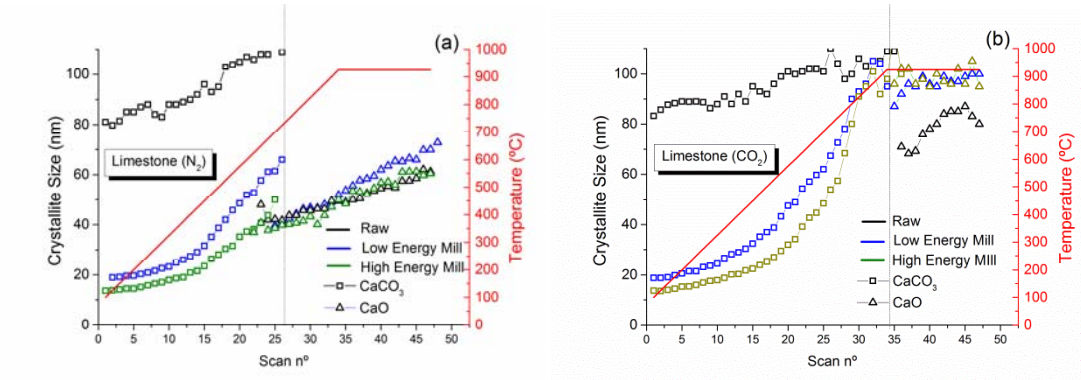

Figure 12. Evolution with temperature of the crystallite size of $CaCO_3$ and CaO during limestone decomposition in (a) N_2 and (b) CO_2, estimated using Lebail method from in-situ XRD measurements for samples of raw and milled limestone at different milling intensities (according to the colour code). The vertical lines are guides to the eye to show the $CaCO_3$ decomposition temperature in each case. Heating rate up to the isotherm is 10ºC/min.

Figure 13a and 13b show the evolution of the crystallite sizes of $CaMg(CO_3)_2$, $CaCO_3$, MgO and CaO along the entire decomposition process of dolomite in N_2 and CO_2 atmospheres, respectively. As in the case of limestone, the crystallite size of dolomite is greatly reduced when subjected to a mechanical pretreatment. It can be observed that the coherent domain size of the formed MgO is about 10 nm irrespective of the atmosphere and the mechanical pretreatment. However, whereas the crystallite growth during calcination in N_2 is negligible, it is somewhat promoted for calcination under CO_2, reaching a size of about 40 nm after 1 hour at 925 ºC. $CaCO_3$ only appears as a result of $CaMg(CO_3)_2$ half-decomposition in CO_2. Nascent $CaCO_3$ is nanocrystalline, with crystallite sizes between 20 and 40 nm, depending on the temperature at which they form. Thus, although the temperature at which $CaCO_3$ forms is moderately reduced by milling, the crystal growth rate does not appear to be strongly influenced by the milling treatment. Note that the growth rate of these nascent $CaCO_3$ crystals is still rather high as it occurred in the case of limestone. Again, this can be explained by the nanocrystalline nature of the milled sorbent in which the numerous grain boundaries favour the sintering by diffusion. Upon decomposition, the nascent CaO nanocrystals appearing from $CaCO_3$ exhibit a crystallite size at the end of the thermal treatment that is larger the more energetic the mechanical grinding imposed to the initial sorbent. On the other hand, it is interesting to note that the crystallite size of MgO, which remains inert to carbonation, is higher for the unmilled sample as opposed to CaO, which upholds the argument that milling promotes solid-state diffusion during the CaCO3 transformation thus leading to the formation of larger and less reactive CaO crystals.

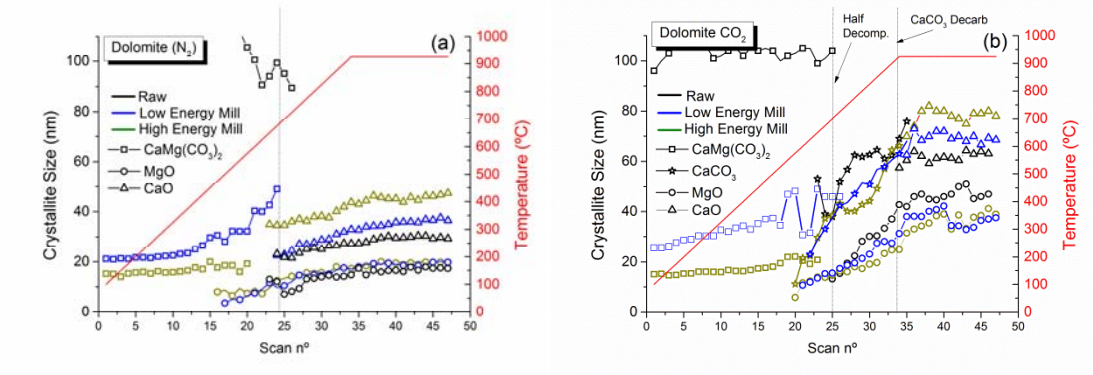

Figura 13. Evolution with temperature of the crystallite size of $MgCa(CO_3)_2$, $CaCO_3$, MgO and CaO during dolomite decomposition in (a) N_2 and (b) CO_2, estimated using Lebail method from in-situ XRD measurements. The vertical lines are guides to the eye to show the temperature for dolomite half-decomposition and the subsequent $CaCO_3$ decomposition. Heating rate up to the isotherm is 10ºC/min.

Therefore, out of the three samples tested, the unmilled dolomite produced the smaller CaO crystals and the SPEX-milled dolomite the larger, independently of the atmosphere in which the experiments were carried out. As argued in the case of lime derived CaO in CO_2 atmosphere, the milled precursors show a higher tendency to sinter thus producing a more crystalline material under the same calcination conditions. The presence of CO_2 proves to have an enormous influence. Thus, while CaO nanocrystals appear in N_2 with a coherent domain length of 20-40 nm, depending on the mechanical treatment, the starting crystallite size of CaO nanocrystals under CO_2 is 60 to 80 nm.

The crystallite size of dolomitic CaO is in all circumstances smaller than lime derived CaO, which can be explained by the hindered sintering effect of the MgO grains. This is consistent with the good capture capacity and cycle repeatability observed for milled dolomite in N_2 [60, 75]. As seen in Figure 13a, milled dolomite calcined in N_2 shows small crystal size and negligible grain growth during the isotherm at 925 ºC while a certain crystal growth is noticeable in lime derived CaO (Figure 12a) without the presence of MgO. Unfortunately, any advantage provided by the low initial crystallinity and high defect concentration of pre-grinded sorbents disappears once the calcinations are carried out in CO_2, in which the sintering of CaO is strongly promoted, as here demonstrated. The crystal size evolution profiles in Figure 13, together with the capture capacities of the different sorbents shown in Figure 8 clearly prove an inverse relationship between crystallinity and capture capacity. The high energy SPEX-milled sorbent yields the largest sized nanocrystalline CaO, which exhibits the lowest carbonation rate whereas the unmilled dolomite, producing the smaller CaO crystals, shows the highest carbonation rate.

4. Conclusions

In this work we have studied the effect of mechanical grinding by ball milling on the multicycle CO_2 capture performance of limestone and dolomite derived CaO at Calcium Looping conditions for CO_2 capture. In an attempt to mimic as closely as possible the operation conditions to be employed in practice, the calcination loops for CaO regeneration have been carried out under high CO_2 partial pressure and at high temperature with fast transitions between calcination and carbonation stages. It has been shown that ball milling has different effects on the CaL capture performance of limestone and dolomite. Whereas the decarbonation rate is significantly enhanced in milled limestone the opposite behaviour is observed in dolomite. However, unlike previous works that reported enhanced capture capacity of milled sorbents, it has been shown here that when calcinations are performed under this harsher conditions, the capture capacity and regenerability of the sorbents are severely hindered. Such behaviour is consistent with the higher tendency to agglomerate and sinter of milled

solids which is even further promoted under the high temperature and high CO_2 environment required in a calciner, thereby producing CaO nanocrystals of much larger size than those obtained from calcination under low CO_2 partial pressure. In-situ XRD calcination analysis clearly reveals the much promoted crystal growth occurring during calcination under CO_2 and the constrained sintering effect provided by MgO particles produced from dolomite half-calcination. Thus, dolomite exhibits improved performance with respect to limestone due to the stabilizing effect provided by the segregated MgO grains forming an inert skeleton that hinders the aggregation and sintering of CaO nanocrystals and mitigates sorbent deactivation. In any case, dolomite, regardless of any previous mechanical treatment, exhibits the ability to fully decarbonate in short residence times at a relatively low temperature of 900ºC as compared to limestone. A decrease of the calcination temperature is critical for a reduction of energy penalty in the CaL process. This may be achieved by mechanical milling, which however hampers the subsequent carbonation activity of the regenerated sorbent as sintering of the milled $CaCO_3$ and nascent CaO nanocrystals is enhanced. As a general conclusion, the results here presented indicate that maintaining the nanocrystalline structure of CaO with crystallite sizes as small as possible after calcination is a key issue to mitigate the loss of multicycle capture capacity.

Acknowledgements

This work was supported by the Andalusian Regional Government Junta de Andalucia (Contracts FQM-5735, TEP-7858 and TEP-1900), Spanish Government Agency Ministerio de Economia y Competitividad and FEDER funds (contracts CTQ2014-52763-C2-2-R and CTQ2014-52763-C2-1-R). One of the authors (PESJ) is supported by by a Marie Curie–Junta de Andalucía Posdoc Talentia grant. The authors also thank VPPI-US for the AP current contract. We gratefully acknowledge the XRD and SEM services of the Innovation, Technology and Research Center of the University of Seville (CITIUS).

Supporting Information description

EDX analysis of milled dolomite, XRD scans measured in-situ during the calcinations for every studied sample, SEM of the cycled sorbents and TGA experiments.

References

(1) Romano, M. C.; Martínez, I.; Murillo, R.; Arstad, B.; Blom, R.; Ozcan, D. C.; Ahn, H.; Brandani, S., Process simulation of Ca-looping processes: review and guidelines. *Energy Procedia* **2013,** 37, 142-150.

(2) Blamey, J.; Anthony, E. J.; Wang, J.; Fennell, P. S., The calcium looping cycle for large-scale CO_2 capture. *Prog. Energ. Combust.* **2010,** 36, 260-279.

(3) Romano, M. C., Modeling the carbonator of a Ca-looping process for CO_2 capture from power plant flue gas. *Chem. Eng. Sci.* **2012,** 69, 257-269.

(4) Arias, B.; Diego, M. E.; Abanades, J. C.; Lorenzo, M.; Diaz, L.; Martínez, D.; Alvarez, J.; Sánchez-Biezma, A., Demonstration of steady state CO_2 capture in a 1.7 MWth calcium looping pilot. *Int. J. Greenh. Gas. Con.* **2013,** 18, 237-245.

(5) Strohle, J.; Junk, M.; Kremer, J.; Galloy, A.; Epple, B., Carbonate looping experiments in a 1 MWth pilot plant and model validation. *Fuel* **2014,** 127, 13-22.

(6) Ylätalo, J.; Ritvanen, J.; Tynjälä, T.; Hyppänen, T., Model based scale-up study of the calcium looping process. *Fuel* **2014,** 115, 329-337.

(7) Hyatt, E. P.; Cutler, I. B.; Wadsworth, M. E., Calcium carbonate decomposition in carbon dioxide atmosphere. *J. Am. Ceram. Soc.* **1958,** 41, 70-74.

(8) Beruto, D.; Barco, L.; Searcy, A. W., CO_2-catalyzed surface-area and porosity changes in high-surface-area cao aggregates. *J. Am. Ceram. Soc.* **1984,** 67, 512-515.

(9) García-Labiano, F.; Abad, A.; de Diego, L. F.; Gayán, P.; Adánez, J., Calcination of calcium-based sorbents at pressure in a broad range of CO_2 concentrations. *Chem. Eng. Sci.* **2002,** 57, 2381-2393.

(10) Khinast, J.; Krammer, G. F.; Brunner, C.; Staudinger, G., Decomposition of limestone: The influence of CO_2 and particle size on the reaction rate. *Chem. Eng. Sci.* **1996,** 51, 623-634.

(11) Valverde, J. M.; Sanchez-Jimenez, P. E.; Perez-Maqueda, L. A., Limestone calcination nearby equilibrium: kinetics, CaO crystal structure, sintering and reactivity. *J. Phys. Chem. C* **2015,** 119, 1623-1641.

(12) Perejón, A.; Romeo, L. M.; Lara, Y.; Lisbona, P.; Martínez, A.; Valverde, J. M., The Calcium-Looping technology for CO2 capture: On the important roles of energy integration and sorbent behavior. *Appl. Energ.* **2016,** 162, 787-807.

(13) Charitos, A.; Rodríguez, N.; Hawthorne, C.; Alonso, M.; Zieba, M.; Arias, B.; Kopanakis, G.; Scheffknecht, G.; Abanades, J. C., Experimental validation of the calcium looping CO_2 capture process with two circulating fluidized bed carbonator reactors. *Ind. Eng. Chem. Res.* **2011,** 50, 9685-9695.

(14) Martínez, I.; Grasa, G.; Murillo, R.; Arias, B.; Abanades, J. C., Modelling the continuous calcination of $CaCO_3$ in a Ca-looping system. *Chem. Eng. J.* **2013,** 215–216, 174-181.

(15) Coppola, A.; Scala, F.; Salatino, P.; Montagnaro, F., Fluidized bed calcium looping cycles for CO2 capture under oxy-firing calcination conditions: Part 1. Assessment of six limestones. *Chem. Eng. J.* **2013,** 231, 537-543.

(16) Rodriguez, N.; Alonso, M.; Grasa, G.; Abanades, J. C., Heat requirements in a calciner of $CaCO_3$ integrated in a CO_2 capture system using CaO. *Chem. Eng. J.* **2008,** 138, 148-154.

(17) Martínez, A.; Lara, Y.; Lisbona, P.; Romeo, L. M., Operation of a cyclonic preheater in the Ca-Looping for CO_2 capture. *Environ. Sci. Technol.* **2013,** 47, 11335-11341.

(18) Ylätalo, J.; Parkkinen, J.; Ritvanen, J.; Tynjälä, T.; Hyppänen, T., Modeling of the oxy-combustion calciner in the post-combustion calcium looping process. *Fuel* **2013,** 113, 770-779.

(19) Martínez, A.; Lara, Y.; Lisbona, P.; Romeo, L. M., Energy penalty reduction in the calcium looping cycle. *Int. J. Greenh. Gas. Con.* **2012,** 7, 74-81.
(20) Borgwardt, R. H., Sintering of nascent calcium-oxide. *Chem. Eng. Sci.* **1989,** 44, 53-60.
(21) German, R. M.; Munir, Z. A., Surface Area Reduction During Isothermal Sintering. *J. Am. Ceram. Soc.* **1976,** 59, 379-383.
(22) Borgwardt, R. H., Calcium oxide sintering in atmospheres containing water and carbon dioxide. *Ind. Eng. Chem. Res.* **1989,** 28, 493-500.
(23) Valverde, J. M.; Sanchez-Jimenez, P. E.; Perez-Maqueda, L. A., Calcium-looping for post-combustion CO_2 capture. On the adverse effect of sorbent regeneration under CO_2. *Appl. Energ.* **2014,** 126, 161-171.
(24) Grasa, G. S.; Abanades, J. C., CO_2 capture capacity of CaO in long series of carbonation/calcination cycles. *Ind. Eng. Chem. Res.* **2006,** 45, 8846-8851.
(25) Fierro, V.; Adánez, J.; García-Labiano, F., Effect of pore geometry on the sintering of Ca-based sorbents during calcination at high temperatures. *Fuel* **2004,** 83, 1733-1742.
(26) Valverde, J. M.; Perejon, A.; Medina, S.; Perez-Maqueda, L. A., Thermal decomposition of dolomite under CO2: Insights from TGA and in situ XRD analysis. *Phys. Chem. Chem. Phys.* **2015,** 17, 30162-30176.
(27) Chen, H.; Zhang, P.; Duan, Y.; Zhao, C., CO2 capture of calcium based sorbents developed by sol-gel technique in the presence of steam. *Chem. Eng. J.* **2016,** 295, 218-226.
(28) Wu, Y.; Blamey, J.; Anthony, E. J.; Fennell, P. S., Morphological Changes of Limestone Sorbent Particles during Carbonation/Calcination Looping Cycles in a Thermogravimetric Analyzer (TGA) and Reactivation with Steam. *Energ. Fuel.* **2010,** 24, 2768-2776.
(29) Donat, F.; Florin, N. H.; Anthony, E. J.; Fennell, P. S., Influence of High-Temperature Steam on the Reactivity of CaO Sorbent for CO2 Capture. *Environ. Sci. Technol.* **2012,** 46, 1262-1269.
(30) Champagne, S.; Lu, D. Y.; Symonds, R. T.; Macchi, A.; Anthony, E. J., The effect of steam addition to the calciner in a calcium looping pilot plant. *Powder Technology* **2016,** 290, 114-123.
(31) Shimizu, T.; Hirama, T.; Hosoda, H.; Kitano, K.; Inagaki, M.; Tejima, K., A Twin Fluid-Bed Reactor for Removal of CO2 from Combustion Processes. *Chem. Eng. Res. Des.* **1999,** 77, 62-68.
(32) Biasin, A.; Segre, C. U.; Strumendo, M., CaCO3 Crystallite Evolution during CaO Carbonation: Critical Crystallite Size and Rate Constant Measurement by In-Situ Synchrotron Radiation X-ray Powder Diffraction. *Crystal Growth and Design* **2015,** 15, 5188-5201.
(33) Valverde, J. M.; Sanchez-Jimenez, P. E.; Perez-Maqueda, L. A., Role of precalcination and regeneration conditions on postcombustion CO_2 capture in the Ca-looping technology. *Appl. Energ.* **2014,** 136, 347-356.
(34) Wang, J.; Manovic, V.; Wu, Y.; Anthony, E. J., A study on the activity of CaO-based sorbents for capturing CO_2 in clean energy processes. *Appl. Energ.* **2010,** 87, 1453-1458.
(35) Valverde, J. M.; Sanchez-Jimenez, P. E.; Perez-Maqueda, L. A.; Quintanilla, M. A. S.; Perez-Vaquero, J., Role of crystal structure on CO_2 capture by limestone derived CaO subjected to carbonation/recarbonation/calcination cycles at Ca-looping conditions. *Appl. Energ.* **2014,** 125, 264-275.
(36) Chen, H.; Zhang, P.; Duan, Y.; Zhao, C., Reactivity enhancement of calcium based sorbents by doped with metal oxides through the sol–gel process. *Appl. Energ.* **2016,** 162, 390-400.
(37) Butler, J. W.; Jim Lim, C.; Grace, J. R., Kinetics of CO2 absorption by CaO through pressure swing cycling. *Fuel* **2014,** 127, 78-87.
(38) Wang, C.; Zhou, X.; Jia, L.; Tan, Y., Sintering of limestone in calcination/carbonation cycles. *Industrial and Engineering Chemistry Research* **2014,** 53, 16235-16244.
(39) Yu, F. C.; Phalak, N.; Sun, Z.; Fan, L. S., Activation strategies for calcium-based sorbents for CO 2 capture: A perspective. *Industrial and Engineering Chemistry Research* **2012,** 51, 2133-2142.
(40) Bouquet, E.; Leyssens, G.; Schönnenbeck, C.; Gilot, P., The decrease of carbonation efficiency of CaO along calcination-carbonation cycles: Experiments and modelling. *Chem. Eng. Sci.* **2009,** 64, 2136-2146.

(41) Rodriguez-Navarro, C.; Ruiz-Agudo, E.; Luque, A.; Rodriguez-Navarro, A. B.; Ortega-Huertas, M., Thermal decomposition of calcite: Mechanisms of formation and textural evolution of CaO nanocrystals. *Am. Miner.* **2009,** 94, 578-593.
(42) Valverde, J. M.; Sanchez-Jimenez, P. E.; Perez-Maqueda, L. A., Effect of heat pretreatment/recarbonation in the Ca-Looping process at realistic calcination conditions. *Energ. Fuel.* **2014,** 28, 4062-4067.
(43) Valverde, J. M.; Sanchez-Jimenez, P. E.; Perejon, A.; Perez-Maqueda, L. A., Constant rate thermal analysis for enhancing the long-term CO_2 capture of CaO at Ca-looping conditions. *Appl. Energ.* **2013,** 108, 108-120.
(44) Valverde, J. M.; Sanchez-Jimenez, P. E.; Perejon, A.; Perez-Maqueda, L. A., Role of looping-calcination conditions on self-reactivation of thermally pretreated CO_2 sorbents based on CaO. *Energ. Fuel.* **2013,** 27, 3373-3384.
(45) Arias, B.; Grasa, G. S.; Alonso, M.; Abanades, J. C., Post-combustion calcium looping process with a highly stable sorbent activity by recarbonation. *Energ. Environ. Sci.* **2012,** 5, 7353-7359.
(46) Grasa, G.; Martínez, I.; Diego, M. E.; Abanades, J. C., Determination of CaO carbonation kinetics under recarbonation conditions. *Energ. Fuel.* **2014,** 28, 4033-4042.
(47) Valverde, J. M.; Sanchez-Jimenez, P. E.; Perez-Maqueda, L. A., High and stable Co2 capture capacity of natural limestone at Ca-looping conditions by heat pretreatment and recarbonation synergy. *Fuel* **2014,** 123, 79-85.
(48) Manovic, V.; Anthony, E. J., Thermal activation of CaO-based sorbent and self-reactivation during CO_2 capture looping cycles. *Environ. Sci. Technol.* **2008,** 42, 4170-4174.
(49) Wang, K.; Hu, X.; Zhao, P.; Yin, Z., Natural dolomite modified with carbon coating for cyclic high-temperature CO2 capture. *Appl. Energ.* **2016,** 165, 14-21.
(50) Qin, C.; Yin, J.; Feng, B.; Ran, J.; Zhang, L.; Manovic, V., Modelling of the calcination behaviour of a uniformly-distributed CuO/CaCO3 particle in Ca-Cu chemical looping. *Appl. Energ.* **2016,** 164, 400-410.
(51) Sanchez-Jimenez, P. E.; Perez-Maqueda, L. A.; Valverde, J. M., Nanosilica supported CaO: A regenerable and mechanically hard CO2 sorbent at Ca-looping conditions. *Appl. Energ.* **2014,** 118, 92-99.
(52) Zhou, Z.; Qi, Y.; Xie, M.; Cheng, Z.; Yuan, W., Synthesis of CaO-based sorbents through incorporation of alumina/aluminate and their CO2 capture performance. *Chem. Eng. Sci.* **2012,** 74, 172-180.
(53) Radfarnia, H. R.; Sayari, A., A highly efficient CaO-based CO2 sorbent prepared by a citrate-assisted sol–gel technique. *Chem. Eng. J.* **2015,** 262, 913-920.
(54) Soria-Hoyo, C.; Valverde, J. M.; Van Ommen, J. R.; Sánchez-Jiménez, P. E.; Pérez-Maqueda, L. A.; Sayagués, M. J., Synthesis of a nanosilica supported CO2 sorbent in a fluidized bed reactor. *Applied Surface Science* **2015,** 328, 548-553.
(55) Shearer, J. A.; Johnson, I.; Turner, C. B., Effects of sodium chloride on limestone calcination and sulfation in fluidized-bed combustion. *Environ. Sci. Technol.* **1979,** 13, 1113-1118.
(56) Reddy, E. P.; Smirniotis, P. G., High-Temperature Sorbents for CO2 Made of Alkali Metals Doped on CaO Supports. *The Journal of Physical Chemistry B* **2004,** 108, 7794-7800.
(57) Manovic, V.; Anthony, E. J., Long-Term Behavior of CaO-Based Pellets Supported by Calcium Aluminate Cements in a Long Series of CO2 Capture Cycles. *Ind. Eng. Chem. Res.* **2009,** 48, 8906-8912.
(58) Wu, S. F.; Li, Q. H.; Kim, J. N.; Yi, K. B., Properties of a Nano CaO/Al2O3 CO2 Sorbent. *Ind. Eng. Chem. Res.* **2008,** 47, 180-184.
(59) Li, C. C.; Wu, U. T.; Lin, H. P., Cyclic performance of CaCO3@mSiO2 for CO2 capture in a calcium looping cycle. *J. Mater. Chem. A* **2014,** 2, 8252-8257.
(60) Sanchez-Jimenez, P. E.; Valverde, J. M.; Perez-Maqueda, L. A., Multicyclic conversion of limestone at Ca-looping conditions: The role of solid-sate diffusion controlled carbonation. *Fuel* **2014,** 127, 131-140.

(61) Valverde, J. M.; Sanchez-Jimenez, P. E.; Perez-Maqueda, L. A., Ca-looping for postcombustion CO_2 capture: A comparative analysis on the performances of dolomite and limestone. *Appl. Energ.* **2015,** 138, 202-215.
(62) Valverde, J. M.; Sanchez-Jimenez, P. E.; Perez-Maqueda, L. A., Relevant influence of limestone crystallinity on CO_2 capture in the Ca-Looping technology at realistic calcination conditions. *Environ. Sci. Technol.* **2014,** 48, 9882-9889.
(63) Wang, Y.; Thomson, W. J., The effects of steam and carbon dioxide on calcite decomposition using dynamic X-ray diffraction. *Chem. Eng. Sci.* **1995,** 50, 1373-1382.
(64) Manovic, V.; Anthony, E. J., Steam Reactivation of Spent CaO-Based Sorbent for Multiple CO2 Capture Cycles. *Environ. Sci. Technol.* **2007,** 41, 1420-1425.
(65) Silaban, A.; Narcida, M.; Harrison, D. P., Characteristics of the reversible reaction between CO_2(g) and calcined dolomite. *Chem. Eng. Commun.* **1996,** 146, 149-162.
(66) Albrecht, K. O.; Wagenbach, K. S.; Satrio, J. A.; Shanks, B. H.; Wheelock, T. D., Development of a CaO-Based CO_2 sorbent with improved cyclic stability. *Ind. Eng. Chem. Res.* **2008,** 47, 7841-7848.
(67) Coppola, A.; Scala, F.; Salatino, P.; Montagnaro, F., Fluidized bed calcium looping cycles for CO_2 capture under oxy-firing calcination conditions: Part 2. Assessment of dolomite vs. limestone. *Chem. Eng. J.* **2013,** 231, 544-549.
(68) Haul, R. A. W.; Heystek, H., Differential thermal analysis of the dolomite decomposition. *Am. Miner.* **1952,** 37, 166-179.
(69) Caceres, P. G.; Attiogbe, E. K., Thermal decomposition of dolomite and the extraction of its constituents. *Miner. Eng.* **1997,** 10, 1165-1176.
(70) Rodriguez-Navarro, C.; Kudlacz, K.; Ruiz-Agudo, E., The mechanism of thermal decomposition of dolomite: New insights from 2D-XRD and TEM analyses. *Am. Miner.* **2012,** 97, 38-51.
(71) Readman, J. E.; Blom, R., The use of in situ powder X-ray diffraction in the investigation of dolomite as a potential reversible high-temperature CO_2 sorbent. *Phys. Chem. Chem. Phys.* **2005,** 7, 1214-1219.
(72) de la Calle Martos, A.; Valverde, J. M.; Sanchez-Jimenez, P. E.; Perejon, A.; Garcia-Garrido, C.; Perez-Maqueda, L. A., Effect of dolomite decomposition under CO2 on its multicycle CO2 capture behaviour under calcium looping conditions. *Phys. Chem. Chem. Phys.* **2016,** 18, 16325-16336.
(73) Jones, W.; Eddleston, M. D., Introductory lecture: Mechanochemistry, a versatile synthesis strategy for new materials. *Faraday Discussions* **2014,** 170, 9-34.
(74) Baláž, P.; Achimovičová, M.; Baláž, M.; Billik, P.; Cherkezova-Zheleva, Z.; Criado, J. M.; Delogu, F.; Dutková, E.; Gaffet, E.; Gotor, F. J.; Kumar, R.; Mitov, I.; Rojac, T.; Senna, M.; Streletskii, A.; Wieczorek-Ciurowa, K., Hallmarks of mechanochemistry: From nanoparticles to technology. *Chemical Society Reviews* **2013,** 42, 7571-7637.
(75) Sayyah, M.; Lu, Y.; Masel, R. I.; Suslick, K. S., Mechanical Activation of CaO-Based Adsorbents for CO2 Capture. *ChemSusChem* **2013,** 6, 193-198.
(76) Dollimore, D.; Dunn, J. G.; Lee, Y. F.; Penrod, B. M., The decrepitation of dolomite and limestone. *Thermochim. Acta* **1994,** 237, 125-131.
(77) Hanak, D. P.; Anthony, E. J.; Manovic, V., A review of developments in pilot-plant testing and modelling of calcium looping process for CO_2 capture from power generation systems. *Energ. Environ. Sci.* **2015,** 8, 2199-2249.
(78) Valverde, J. M.; Quintanilla, M. A. S., Attrition of Ca-based CO2-adsorbents by a high velocity gas jet. *AIChE J.* **2013,** 59, 1096-1107.
(79) Bradley, W. F.; Burst, J. F.; Graf, D. L., CRYSTAL CHEMISTRY AND DIFFERENTIAL THERMAL EFFECTS OF DOLOMITE. *Am. Miner.* **1953,** 38, 207-217.
(80) Arai, Y.; Yasue, T., Mechanochemistry of Dolomite. *Gypsum & Lime* **1970,** 1970, 17-23.
(81) Arai, Y., *Chemistry of Powder Production*. 1 ed.; Springer Netherlands: 1996.

(82) Romeo, L. M.; Lara, Y.; Lisbona, P.; Martínez, A., Economical assessment of competitive enhanced limestones for CO_2 capture cycles in power plants. *Fuel Process. Technol.* **2009,** 90, 803-811.
(83) Valverde, J. M.; Sanchez-Jimenez, P. E.; Perejon, A.; Perez-Maqueda, L. A., CO_2 multicyclic capture of pretreated/doped CaO in the Ca-looping process. Theory and experiments. *Phys. Chem. Chem. Phys.* **2013,** 15, 11775-11793.
(84) Voigts, F.; Bebensee, F.; Dahle, S.; Volgmann, K.; Maus-Friedrichs, W., The adsorption of CO2 and CO on Ca and CaO films studied with MIES, UPS and XPS. *Surf. Sci.* **2009,** 603, 40-49.
(85) Ochs, D.; Braun, B.; Maus-Friedrichs, W.; Kempter, V., CO2 chemisorption at Ca and CaO surfaces: a study with MIES, UPS(HeI) and XPS. *Surf. Sci.* **1998,** 417, 406-414.
(86) Bhatia, S. K.; Perlmutter, D. D., Effect of the product layer on the kinetics of the CO_2-lime reaction. *AIChE J.* **1983,** 29, 79-86.
(87) Sun, Z.; Luo, S.; Qi, P.; Fan, L.-S., Ionic diffusion through Calcite ($CaCO_3$) layer during the reaction of CaO and CO_2. *Chem. Eng. Sci.* **2012,** 81, 164-168.
(88) Grasa, G.; Murillo, R.; Alonso, M.; Abanades, J. C., Application of the random pore model to the carbonation cyclic reaction. *AIChE J.* **2009,** 55, 1246-1255.
(89) Mess, D.; Sarofim, A. F.; Longwell, J. P., Product Layer Diffusion during the Reaction of Calcium Oxide with Carbon Dioxide. *Energ. Fuel.* **1999,** 13, 999-1005.
(90) Heitjans, P.; Indris, S., Fast diffusion in nanocrystalline ceramics prepared by ball milling. *J. Mater. Sci.* **2004,** 39, 5091-5096.
(91) Liu, M.; Evans, B., Dislocation recovery kinetics in single-crystal calcite. *Journal of Geophysical Research: Solid Earth* **1997,** 102, 24801-24809.
(92) Kronenberg, A.; Yund, R.; Giletti, B., Carbon and oxygen diffusion in calcite: Effects of Mn content and P H_2O. *Phys. Chem. Minerals.* **1984,** 11, 101-112.
(93) Anderson, T. F., Self-diffusion of carbon and oxygen in calcite by isotope exchange with carbon dioxide. *J. Geophys. Res.* **1969,** 74, 3918-3932.
(94) Arai, Y., *Chemistry of Power Production*. ed.; Chapman & Hall: Glasgow, 1996.
(95) Gammage, R. B.; Glasson, D. R.; Hodgson, I. R.; O'Neill, P., Microcrystalline structure of milled dolomite and its constituent carbonates. *Journal of Colloid And Interface Science* **1983,** 92, 530-544.
(96) Butler, J. W.; Lim, C. J.; Grace, J. R., CO2 capture capacity of CaO in long series of pressure swing sorption cycles. *Chem. Eng. Res. Des.* **2011,** 89, 1794-1804.

For Table of Contents Use Only

Influence of ball milling on CaO crystal growth during limestone and dolomite calcination: Effect on CO_2 capture at Calcium Looping conditions.

Pedro E. Sánchez-Jiménez[2,], José M. Valverde[2], Antonio Perejón[1,3], Antonio de la Calle[1, 2] , Santiago Medina[4] and Luis A. Pérez-Maqueda[1]*

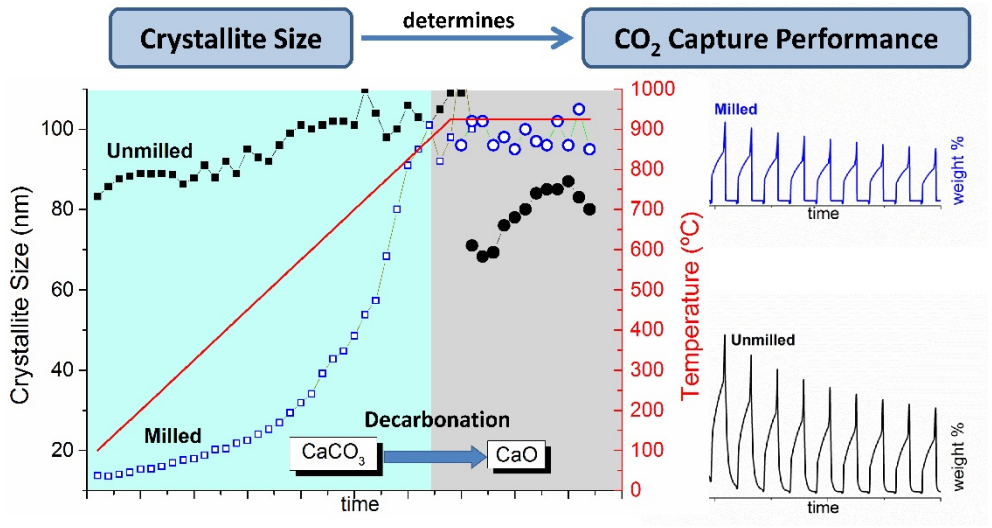

Synopsis

Under Calcium-Looping "realistic" operation conditions (high CO_2 concentration and temperature) the multicycle CO_2 capture capacity performance of CaO derived from limestone and dolomite is inversely related to its crystallite size. Ball-milling the raw sorbents results in the formation of larger nascent CaO nanocrystals during the calcination. Constraint sintering effect due to inert compounds such as dolomitic MgO mitigates the inactivation.

[*]Pedro E. Sánchez Jiménez
Instituto de Ciencia de Materiales de Sevilla,
C. Américo Vespucio nº49, 41092 Sevilla, Spain
Tel +34954489548 Fax +34954460665
e-mail address: pedro.enrique@icmse.csic.es